# GRAPHITE FOAM THERMOSYPHON EVAPORATOR PERFORMANCE OPTIMIZATION: EFFECTS OF WORKING FLUID, LIQUID LEVEL, AND CHAMBER PRESSURE

Johnathan S. Coursey
University of Maryland
Department of Mechanical Engineering
College Park, Maryland 20742 USA
E-mail: jcoursey@wam.umd.edu

Hongkoo Roh
University of Maryland
Department of Mechanical Engineering
College Park, Maryland 20742 USA
E-mail: hkroh@eng.umd.edu

Jungho Kim
University of Maryland
Department of Mechanical Engineering
College Park, Maryland 20742 USA
E-mail: kimjh@eng.umd.edu

Paul J. Boudreaux
Laboratory for Physical Sciences
College Park, Maryland 20740 USA
E-mail: boudreau@eng.umd.edu

## ABSTRACT

Graphite foams have recently been developed at ORNL and are beginning to be applied to thermal management of electronics. These foams consist of a network of interconnected graphite ligaments whose thermal conductivities are up to five times higher than copper. The thermal conductivity of the bulk graphite foam is similar to aluminum, but graphite foam has one-fifth the density of aluminum. This combination of high thermal conductivity and low density results in a thermal diffusivity about four times higher than that of aluminum, allowing heat to rapidly propagate into the foam. This heat is spread out over the very large surface area within the foam, enabling large amounts of energy to be transferred with relatively low temperature difference. The use of graphite foam as the evaporator of a thermosyphon is investigated due to its potential to transfer large amounts of energy without the need for external pumping. A preliminary optimization of the parameters governing evaporator performance is performed using 2-level factorial design. Performance of the system with both PF-5060 and PF-5050 were examined as well as the effects of liquid level and chamber pressure.

## NOMENCLATURE

| | |
|---|---|
| $H$ | Relative height of the graphite foam sample |
| $T$ | Temperature [°C] |
| $T_w$ | Wall temperature [°C] |
| $dT/dz$ | Temperature gradient in the neck of the heating block [K/cm] |
| $f_i$ | Fraction of data values |
| $k_{OHFC}$ | Thermal conductivity [W/cm·K] |
| $n$ | Number of observations |
| $q_{0.1}$ | Normal quantile |
| $\dot{q}''$ | Heat flux at the copper/graphite interface [W/cm$^2$] |
| $r_i$ | Result of the $i^{th}$ trial [W/cm$^2$] |
| $w_j$ | Main effect of the $j^{th}$ parameter |
| $w_{jk}$ | Interaction effect of the $j^{th}$ and $k^{th}$ parameters |
| $x_j$ | $j^{th}$ parameter |

Greek

| | |
|---|---|
| $\Delta$ | Uncertainty of a given parameter |
| $\rho_{rel}$ | Relative density |

## INTRODUCTION

The microprocessor market is driven by the desire for higher performance and decreased size. Meeting these demands requires constantly increasing power density. Intel predicts that high performance next-generation processors will demand about 40 W/cm$^2$ [1] This high thermal design heat flux is necessary because lower operating temperatures ensure reliability goals are met and result in reduced gate delay and higher microprocessor speed. Typically, 85 °C is considered the thermal design temperature limit for high performance electronics. Therefore, the effective thermal management solution must be able to dissipate a high heat flux while remaining at a low chip temperature.

One way to manage this thermal load is with a thermosyphon. A two-phase closed thermosyphon consists of an evaporator, a condenser, and an adiabatic section that allows a working fluid to travel between the other two components. Vapor generated at the evaporator rises due to buoyancy effects. It then condenses at the top of the chamber at the condenser, releasing its latent heat. Finally, gravity returns the condensate back to the evaporator, and the process repeats [2]. Heat generated by a microprocessor could be transferred to the evaporator of a thermosyphon that is bonded with a thin thermally conductive

interface to the backside of the chip, using standard flip-chip design. At the evaporator, heat would vaporize a working fluid such as FC-72, and ultimately, heat would be dissipated at the condenser.

Much research has been done on enhanced evaporators for electronic cooling. Ramaswamy et al. [3, 4] and Pal et al. [5] have investigated the performance of copper enhanced-microstructure thermosyphons and have seen heat transfer rates up to 100 W/cm$^2$. These investigations utilize an enhanced evaporator consisting of a stack of six copper plates, which are grooved with rectangular microchannels. Ramaswamy et al. [3] found that systems operating at partial vacuum result in higher heat fluxes than pressurized systems. In another study, Ramaswamy et al. [4] found that evaporator confinements rendering gaps as small as 1.5 mm are acceptable and result in an acceptably small deterioration in performance. Other researchers, such as Mudawar and Anderson [6, 7], have examined the pool boiling performance of fluorinerts on enhanced copper studs and microgrooves and have achieved heat fluxes of about 105 W/cm$^2$ while maintaining the surface temperature below 85 °C. They found that increased pressures result in higher critical heat flux (CHF) but at much higher wall temperatures. Furthermore, they found subcooling to dramatically increase CHF and reduce wall temperature. Their study of performance variation among working fluids indicates that FC-72 is ideal in most circumstances but that FC-87's lower boiling point make it ideal for heavily finned surfaces. These studies of copper enhanced-microstructure evaporators have achieved four-fold increases over the heat dissipation capability of bare copper with pool boiling. To achieve even higher enhancements, other materials and microstructures must be considered.

Another potentially effective thermosyphon design is one made from pitch-derived carbon foam. This carbon foam developed by James Klett at Oak Ridge National Laboratory (ORNL) is an ideal thermal management material because it has a low density, high thermal diffusivity, and a coefficient of thermal expansion that is close to that of silicon. Some properties of the graphite foam used in this investigation (Poco Graphite, Inc.) are shown in Table 1. Thermosyphon evaporator performance is governed largely by the thermal diffusivity of the material used. While most low density materials have a low thermal diffusivity, graphite foam has a remarkably high thermal diffusivity as shown in Table 2.

| Property | Value |
|---|---|
| Pore diameter (average) | 350 μm |
| Specific area | > 4 m$^2$/g |
| Open porosity | > 96% |
| Total porosity | 73 – 82% |
| Density | 0.2 – 0.6 g/cm$^3$ |
| Thermal conductivity | 100 – 150 W/m-K |
| Specific heat | 0.70 J/g-K |
| Thermal diffusivity | 3.71 cm$^2$/s |
| Coefficient of thermal expansion | 2 – 3 μm/m-K |
| Compressive strength (when density = 0.5 g/cm$^3$) | 2.07 MPa |

Table 1. PocoFoam properties [8].

| Material | Density [g/cm$^3$] | Thermal Diffusivity [cm$^2$/s] |
|---|---|---|
| Graphite foam[8] | 0.50 | 3.71 |
| Silver (pure) | 10.5 | 1.74 |
| Silver foam ($\rho_{rel}$ = 10%)[9] | 1.04 | 0.33 |
| Copper (pure) | 8.933 | 1.17 |
| Copper foam ($\rho_{rel}$ = 10%)[9] | 0.9 | 0.22 |
| Aluminum (pure) | 2.702 | 0.97 |
| Aluminum foam[10] | 0.5 | 0.27 |

Table 2. Thermal diffusivities of various materials.

The purpose of this investigation is to gain a preliminary understanding of the effects of three parameters that are key to the performance of a graphite foam thermosyphon evaporator. The effects of working fluid, liquid level, and chamber pressure were determined by generating boiling curves for the nucleate boiling regime. Other parameters such as heater size, geometry, pore size, density, and foam orientation were held constant. With an understanding of the effects of these three parameters, optimized working fluid, liquid level, and chamber pressure can be used in further parameterization studies.

## EXPERIMENTAL SETUP

A diagram of the experimental rig used for this study is shown in Fig. 1.

**Enclosure.** The heating block and the G10 insulation are held inside the aluminum housing, which is 108 mm high and 203 mm in outer diameter. The Lexan chamber (102 mm high and 152 mm in diameter) is epoxied to the housing to form the transparent walls of the test rig. The top of the chamber is closed by the aluminum lid, which is pressed down on to the chamber by bolts and sealed with a foam rubber gasket.

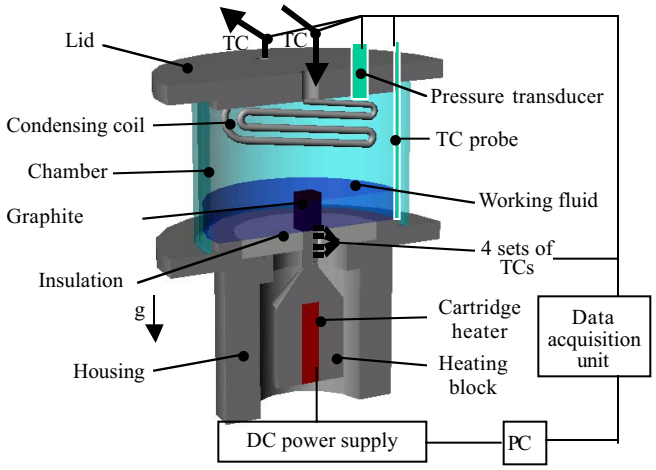


Figure 1. Experimental setup.

**Graphite Foam.** A photograph of the graphite foam is shown in Figure 2. The graphite foam was milled into a rectangular sample 18 mm (H) x 13 mm (W) x 13 mm (D). The graphite foam was brazed to the top of the copper heating block by Materials Resources International (Lansdale, PA) using their S-Bond™ process. The brazing is made at relatively low temperatures (<250 °C) and is capable of providing a low thermal resistance interface between the graphite foam and common materials such as copper and aluminum.

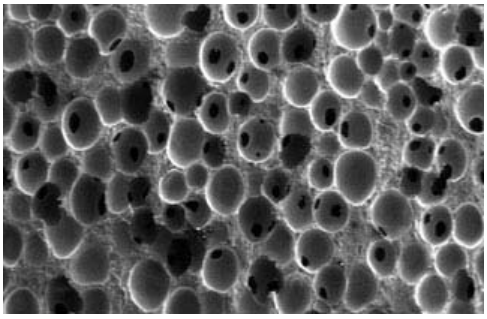

Figure 2. Photograph of graphite foam (Courtesy of James Klett, ORNL).

**Heat Source.** The graphite sample was heated by a 1 $cm^2$ heating surface. Heat was provided by a 500 W cartridge heater embedded within an oxygen free high conductivity (OFHC) copper heating block. The neck of the heating block was designed by computational heat transfer and is insulated to create a one dimensional heat flux. To determine this heat flux, a type T thermocouple is fixed with epoxy into each of four holes (1.3 mm-diameter, 6.4 mm separation) located in the neck of the copper column.

**Working Fluid.** Both PF-5060 and PF-5050 (95% pure FC-72 and FC-87, respectively) were used. These fluids are thermally and chemically stable and were chosen because of their frequent use in thermal management systems. Mudawar and Anderson [6] also found these to be the most effective of the fluorinerts as mentioned above. These fluids also provide a range of boiling points. At one atmosphere, FC-72 boils at 56 °C and FC-87 boils at 30 °C [11, 12]. Both fluids were degassed before each trial, and their bulk temperature near the boiling surface was measured with a type T thermocouple probe.

**Chamber Pressure.** The chamber pressure was varied by controlling the temperature of the water inside the condenser tube. Water from the tap provided a nominally constant condenser temperature, however the inlet and outlet temperatures of the water in the condenser were recorded so exact temperatures could be determined. The chamber pressure was measured by a thin film, millivolt output pressure sensor.

**Control System.** Data acquisition and heating control was provided by a custom Visual C++ program implemented through a general programming interface bus (GPIB) on a Pentium III personal computer (PC). A HP6675A DC power supply provided a controllable power source, while a Fluke Hydra Data Acquisition Unit acquired data from all pressure and temperature channels every three seconds.

## EXPERIMENTAL METHOD

Initially, the goal of this investigation was to determine CHF for eight configurations given by a 2-level factorial design of the three parameters. However, the temperatures required to reach CHF were discovered to be too high for safe operation of the experimental system. An average temperature of 140 °C for the neck of the heating block was set as the temperature limit and experiments were concluded when this limit was reached. The goal of the investigation then shifted to the determination of the highest heat flux possible while remaining below 85 °C, the thermal design limit for high performance electronics.

For a 2-level factorial design experiment given three parameters, a total of eight trials are necessary to completely explore the parameter space. This method assumes linear relationships and is largely a preliminary screening tool. PF-5060 and PF-5050 were used as the extreme conditions for performance fluid; the liquid level was set at the height of the graphite foam sample, *H*, and at one half its height; and the chamber pressure was controlled by setting the condenser temperature to nominal values of 43.5 °C and 23 °C. The experimental test matrix used in this investigation is shown in Table 3.

Transient data were recorded approximately every three seconds throughout the experiment. When steady-state was reached, 60 seconds of steady-state data were acquired, which yielded approximately 20 data points. The criterion for determination of steady-state required that the average temperature in the neck of the heating block change by less than 0.1 K over a 60 second period. Transient temperature data for the neck of the heating block confirm that the heat flux was sufficiently steady. However, during data analysis it was observed that the bulk temperature often increased until it reached a steady-state value well into the experiment. This effect is serious for the high condenser temperature trials and indicates that the condenser capacity was insufficient. Therefore, many of the data points where the heat flux was "steady" were discarded because the bulk temperature had not attained steady-state. Only data points representing an entirely steady system were retained.

| Trial | Working Fluid | Liquid Level | Condenser Temperature [°C] |
|---|---|---|---|
| 1 | PF-5060 | 1/2*H* | 23 |
| 2 | PF-5060 | 1/2 *H* | 43.5 |
| 3 | PF-5060 | *H* | 43.5 |
| 4 | PF-5060 | *H* | 23 |
| 5 | PF-5050 | 1/2 *H* | 23 |
| 6 | PF-5050 | 1/2 *H* | 43.5 |
| 7 | PF-5050 | *H* | 43.5 |
| 8 | PF-5050 | *H* | 23 |

Table 3. Experimental test matrix.

To determine the wall temperature, the temperature gradient in the neck of the heating block was determined by performing a least-squares fit of the temperature measurements from the four thermocouples in the neck and extrapolating to the wall. The heat flux at the wall was determined using Fourier's law assuming a constant thermal conductivity of OFHC copper of 3.867 W/cm-K.

## UNCERTAINTY ANALYSIS

The standard deviations in the heat flux results were calculated using the sum of squares method:

$$\Delta \dot{q}'' = \sqrt{\left(\frac{dT}{dz}\Delta k\right)^2 + \left(k\Delta\frac{dT}{dz}\right)^2} \qquad (1)$$

The copper rod used for the heating block was an OFHC copper of unknown origin. A constant thermal conductivity of 3.867 W/cm-K was assumed and was calculated by determining the average temperature dependent conductivity over the range of temperatures seen in this study using the temperature dependent relationship given by Kedzierski [13]:

$$k_{OFHC} = 78.113 e^{74.924/T} (\ln T)^{0.7842} \qquad (2)$$

The standard deviation associated with this constant thermal conductivity was estimated to be 3.2% based on the uncertainty of the model and the range of temperatures. The standard deviation of the temperature gradient was calculated from the uncertainty of the linear regression. The standard deviation of the temperature gradient was calculated at every time step and in general was found to be larger at higher temperature gradients. The standard deviations were combined according to Eq. 1, and the standard deviation of the heat flux was determined at every time step. The maximum standard deviation of the steady-state heat flux was found to be 2.6 W/cm$^2$, which occurred at the highest heat flux. The minimum standard deviation occurred at the lowest heat flux and was found to be 0.2 W/cm$^2$. The average standard deviation of the heat flux was 1.6 W/cm$^2$.

The standard deviation in the temperature measurements was estimated to be 1.35 °C based on standard accuracies of type T thermocouples and the specifications of the Hydra DAQ Unit.

Uncertainties for the specified conditions were also estimated. The standard deviations in the condenser temperatures were found to be 2.4 °C for the low temperature and 1.7 °C for the high temperature based on the accuracy of the thermocouple measurement and direct inspection of the measured data. The standard deviation in the liquid level was estimated to be 0.5 mm. The standard deviation in the geometry of the graphite foam sample was estimated to be 0.5 mm.

## RESULTS AND DISCUSSION

The results of the eight trials are shown in Fig. 3. Each of the curves shown below was fit using the method of least-squares, and the heat flux was determined for a wall temperature of 85 °C. The results are shown below in Table 4.

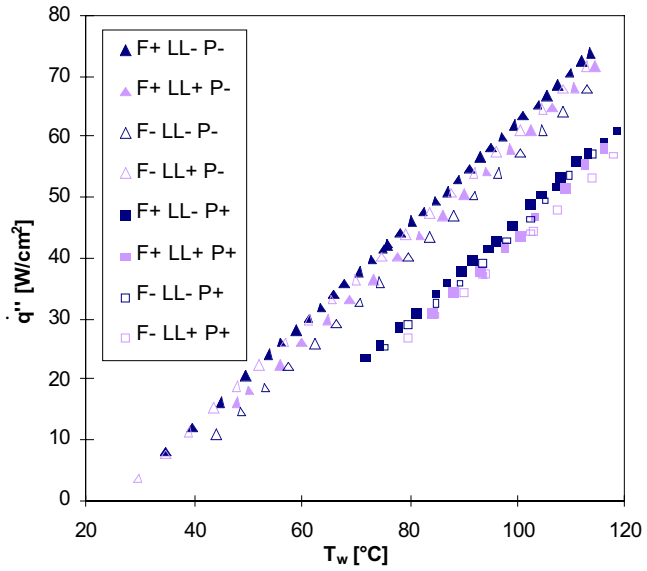


Figure 3. Nucleate boiling curves. F+ (PF-5060), F- (PF-5050), LL+ (high liquid level), LL- (low liquid level), P+ (high pressure), and P- (low pressure).

To determine the dependence of the results on the parameters, the statistical effects were determined. The effects are defined as the difference between the mean response at high and low levels. The main effect, $w_j$, for a parameter $x_j$ is given by:

$$w_j = \frac{\sum_{i=1}^{8} \text{sign}_{ij} r_i}{4} \qquad (3)$$

The interaction effect, $w_{jk}$, for parameters $x_j$ and $x_k$, is given by:

$$w_{jk} = \frac{\sum_{i=1}^{8} \text{sign}_{ij}\text{sign}_{ik} r_i}{4} \qquad (4)$$

| Trial $i$ | Working Fluid ($x_1$) | Liquid Level ($x_2$) | Condenser Temperature ($x_3$) | Result ($r_i$) [W/cm$^2$] |
|---|---|---|---|---|
| 1 | + | - | - | 49.9 |
| 2 | + | - | + | 34.1 |
| 3 | + | + | + | 46.6 |
| 4 | + | + | - | 31.2 |
| 5 | - | - | - | 44.7 |
| 6 | - | - | + | 32.7 |
| 7 | - | + | + | 48.8 |
| 8 | - | + | - | 30.5 |

Table 4. Heat flux results at $T_w$ = 85 °C.

| Parameter | Effect |
|---|---|
| $x_1$ | 1.3 |
| $x_2$ | -1.1 |
| $x_3$ | -15.4 |
| $x_1x_2$ | -2.0 |
| $x_1x_3$ | -0.2 |
| $x_2x_3$ | -1.5 |
| $x_1x_2x_3$ | 1.7 |

Table 5. The effects of working fluid, liquid level, and chamber pressure.

The calculated effects are shown in Table 5. The significance of effects from unreplicated 2-level factorial experiments can be seen in a diagnostic plot such as the normal quantile-quantile plot. In this plot, the $n$ ordered effects are plotted versus the normal quantile function with a mean of zero and standard deviation of one, $q_{0,1}$.

$$q_{0,1}(f_i) \approx 4.91\left(f_i^{0.14} - (1-f_i)^{0.14}\right) \quad (5)$$

$$f_i = \frac{i - 0.375}{n + 0.25} \quad (6)$$

For a normal distribution this yields a straight line. Therefore, those effects that lie on the line are independent estimates of the mean, and are not real effects. Those effects that lie off the line are significant. The slope of the line is an estimate of the standard deviation [14]. The normal quantile-quantile plot of the effects is shown in Fig. 4.

Pressure, $x_3$, is clearly a significant parameter with an effect eight times the standard deviation. The other parameters and the interactions have minor effects over the range of conditions investigated. Lower pressures result in significantly higher heat fluxes, while other parameters cause little variation.

The significant pressure effect was expected based on the results seen by Ramaswamy et al. [3] since it increases the saturation temperature, which delays the onset of nucleate boiling. With a more effective condenser and lower pressure, more heat is removed from the evaporator and higher heat fluxes are observed at relatively low wall temperatures. Higher pressures may result in an increased CHF as other researchers have noted, but CHF is

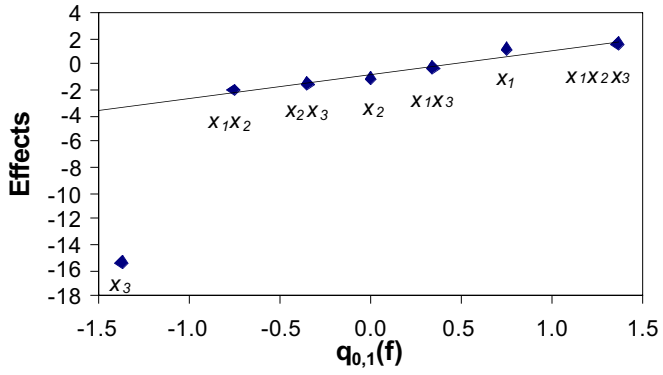


Figure 4. Normal quantile-quantile plot.

well above the 85 °C temperature limit for the geometry and conditions used in this study.

The lack of a significant liquid level effect over the range of investigation was a surprising result. However, the large surface area of the graphite foam and the wetting nature of the fluorinerts results in the foam acting like a sponge that wicks the fluid into the entire foam volume. If the entire surface area is wetted, evaporation can occur over the entire volume regardless of liquid level. In fact, it was observed that higher liquid levels decreased performance. This might be explained by the fact the hydrostatic pressure is higher when the fluid level is increased. This results in decreased boiling performance closer to the wall, and the net effect is a lower total heat flux. Clearly, there is some lower limit to decreasing the liquid level and the effect of submerged boiling is still unknown.

Working fluid, FC-72 or FC-87, was also found not to be a significant factor given the sample used. This result is not surprising given the similar nature of the two fluids. PF-5060 was found to be slightly superior, with better results in three of the four trials. However, it should be noted that the effect of working fluid most likely has a strong interaction with pore size, which is another parameter that will be investigated in the future. Furthermore, no thermal excursion was observed with either fluid.

## CONCLUSIONS

The use of graphite foam as the evaporator in a thermosyphon for the cooling of electronics shows significant promise. This preliminary investigation has shown that heat fluxes approaching 50 W/cm$^2$ while maintaining the wall temperature below 85 °C are possible with little optimization. This study began part of the optimization that is expected to increase this heat flux significantly. It has been determined that lower pressures result in significantly higher heat fluxes. Surprisingly, liquid height does not appear to be a significant factor over the range of heights studied, and will be the focus of further investigation. It was also determined that thermosyphon performance is not significantly different when the working fluid is changed from PF-5060 to PF-5050, although results may vary for foams with different pore sizes. These results will be used to design a more comprehensive parameterization study that will investigate pore size, geometry, and other effects as the limits of graphite foam evaporator performance is explored.

## ACKNOWLEDGMENTS

This project was supported by the Laboratory for Physical Sciences under Grant #MDA90499C2618. The graphite foam samples were provided by Poco Graphite, Inc.

## REFERENCES

[1] Viswanath, R., Wakharkar, V., Watwe, A., and Lebonheur, V., 2000, "Thermal Performance Challenges from Silicon to Systems," Intel Technology Journal, Q3.

 

[2] Faghri, A., 1995, *Heat Pipe Science and Technology*, Taylor and Francis: Washington.

[3] Ramaswamy, C., Joshi, Y., Nakayama, W., 2000, "Combined Effects of Sub-Cooling and Operating Pressure on the Performance of a Two-Chamber Thermosyphon," *IEEE* Transactions on Components and Packaging Technologies, pp. 61-69.

[4] Ramaswamy, C., Joshi, Y., Nakayama, W., and Johnson, W. B., 1999, "Thermal Performance of a Compact Two-phase Thermosyphon: Response to Evaporator Confinement and Transient Loads," Enhanced Heat Transfer, **6**, 279 – 288.

[5] Pal, A., Joshi, Y., Beitelmal, M. H., Patel, C. D., and Wenger, T., 2002, "Design and Performace Evaluation of a Compact Thermosyphon," THERMES 2002, January 13-16, Santa Fe, USA.

[6] Mudawar, I. and Anderson, T. M., 1989, "High Flux Electronic Cooling by Means of Pool Boiling – Part I: Parametric Investigation of the Effects of Coolant Variation, Pressurization, Subcooling, and Surface Augmentation," Heat Transfer in Electronics, ASME HTD-Vol. 111, Ed. R. K. Shah, pp. 25 – 34.

[7] Mudawar, I. and Anderson, T. M., 1989, "High Flux Electronic Cooling by Means of Pool Boiling – Part II: Optimization of Enhanced Surface Geometry," Heat Transfer in Electronics, ASME HTD-Vol. 111, Ed. R. K. Shah, pp. 35 – 49.

[8] Poco Graphite Foam, "Properties Data Sheet," Online: http://www.pocofoam.com/Library/techdata.pdf. Accessed: March 25, 2002.

[9] Porvair Fuel Cell Technology, "Application Properties," Online: http://www.porvair.com/pfc/properties.htm. Accessed: March 28, 2002.

[10] Klett, J. and Conway, B., 2000, "Thermal Management Solutions Utilizing High Thermal Conductivity Graphite Foams," Proceedings of the 45th International SAMPE Symposium and Exhibition, Long Beach, CA, May 21-25, 2000.

[11] 3M, "Fluorinert Electronic Liquid FC-72 Product Information," Online: http://www.3m.com. Accessed: April 5, 2002.

[12] 3M, "Fluorinert Electronic Liquid FC-87 Product Information," Online: http://www.3m.com. Accessed: April 5, 2002.

[13] Kedzierski, M., Private Communication. February, 25, 2002.

[14] Wapole, R. E., Myers, R. H., and Myers, S. L., 1998, *Probability and Statistics for Engineers and Scientists*, Prentice Hall: Upper Saddle River, New Jersey, pp. 211-215,564-565.